ELSEVIER

Journal of Alloys and Compounds 262–263 (1997) 287–291

Journal of ALLOYS AND COMPOUNDS

Electrical conductivity of chromia-pillared α-zirconium phosphate

J.R. Ramos-Barrado[a,*], F. Martín[a], F.J. Pérez-Reina[b], P. Maireles-Torres[b], P. Olivera-Pastor[b], E. Rodríguez-Castellón[b], A. Jiménez-López[b]

[a] *Departamento de Física Aplicada, Facultad de Ciencias, Universidad de Málaga, 29071 Málaga, Spain*
[b] *Departamento de Química Inorgánica, Cristalografía y Mineralogía, Facultad de Ciencias, Universidad de Málaga, 29071 Málaga, Spain*

Abstract

Pillaring of the layered structure of α-zirconium phosphate by chromium(III) oxide has been performed by a new method involving preswelling of the layered substrate by *n*-propylamine vapours, followed by a colloidisation in a pH controlled medium, chromium(III) oligomer grafting and calcination in N_2 at 673 K. Pure chromia-pillared α-zirconium phosphate and Li^+-exchanged derivatives presented enhanced electrical conductivity in comparison with pristine α-zirconium phosphate and much lower activation energies. © 1997 Elsevier Science S.A.

Keywords: Electrical conductivity; Pillared; Zirconium phosphate; Chromium oxide

1. Introduction

Pillared layered solids are formed by intercalation of large polymeric inorganic cations in the interlayer region of layered solids such as clay minerals or layered phosphates [1,2]. After calcination in air or in a controlled atmosphere, the precursor cations are transformed to the respective metal oxide nanoclusters, which prop the layers permanently apart. These metal (Zr, Cr, Al, Ga) oxides interact strongly with the layers giving thermally stable materials of high surface area and pore volume accessible for ion exchange, adsorption, and catalysis [3–6]. Pillared layered phosphates present poor crystallinity, their pore-size distribution is usually quite narrow with high residual cationic exchange capacity, allowing the presence of mobile exchangeable cations and making possible the existence of ionic conductivity. A systematic study of the electrical properties of several alumina-pillared α-M(IV) phosphates (where M = Zr, Sn) has been undertaken [7–10]. Their electrical behaviour can be fitted by supposing two contributions resulting from the existence of two kinds of pores, interlayer micropores and small mesopores induced by pillaring, and mesopores resulting from edge-face interaction between layer packets. Recently, the conducting and dielectric properties of lithium-exchanged mixed Fe-Cr oxide-pillared α-zirconium phosphate has been investigated [11]. The Li^+ ion distribution shows a two potential-well system associated with the two kind of pores, showing a strong dependence on lithium content of the conducting and dielectric properties. The aim of this paper is to study the

* Corresponding author.

0925-8388/97/$17.00
PII S0925-8388(97)00401-5

electrical behaviour of a chromia-pillared α-zirconium phosphate prepared by a novel method that gives rise to a more ordered structure.

2. Materials and experimental methods

2.1. Preparation of lithium-exchanged chromia pillared layered zirconium phosphate

α-Zirconium phosphate, α-ZrP, was prepared following the method described elsewhere [12]. Subsequently, 2 g of α-ZrP were preswelled with *n*-propylamine vapours overnight. This material was dispersed in 0.026 M acetic acid (400 ml), resulting in a suspension presenting a pH = 5. Later, 0.1 N *n*-propylamine was added up to pH = 8, in order to start the polymerisation of the Cr(III) species.

The above suspension was mixed with a $Cr(OAc)_3$ solution. The final concentration of Cr(III) was 0.031 M. Later, the suspension was refluxed for 4 days, giving rise to a precursor material with a $d_{(001)} = 44.0$ Å (Fig. 1). Finally, the solid which was calcined in N_2 at 673 K, presents a very high interlayer distance, $d_{(001)} = 30.0$ Å, with a high specific surface area (426 $m^2\ g^{-1}$) and a narrow pore size distribution (Fig. 2b). As zeolites, pillared phosphate materials show cationic exchange properties owing to the remain ıg not neutralized POH groups of the layered phosphate. So, the chromia pillared compound was fully ion-exchanged with 0.05 M LiOH solution.

2.2. Physical measurements

Pellets of 13 mm in diameter and 1 mm thickness were prepared at 6 MPa. Opposite faces of disc-shaped samples were coated with gold by a vapour deposition method. The dc current conductivity was measured by means of a PAmeter/D C. Voltage Source HP4140B controlled by computer. The ac electrical behaviour of the pellet was performed using a Solartron 1260, controlled by computer also. The electrical response was measured in the range between 1 Hz and 5 MHz. The temperature range was between 484 K and 972 K, and it was measured by means of a platinum thermometer; the temperature did not change more than 1% during the measurement. The experimental data were corrected by software and the influence of connecting cables and other parasite capacitances were eliminated.

3. Results and discussion

Pure chromia-pillared α-zirconium phosphate presents a high electronic conductivity ($3 \times 10^{-4}\ \Omega^{-1}$ cm at 845 K) which may be measured by the dc method. This conductivity is higher than that of other oxide-pillared phosphates (10^{-5}–$10^{-9}\ \Omega^{-1}$ cm) [7–10]. There is no appreciable change of dc intensity vs. time for that sample; however, the Li^+-exchanged derivative sample is a mixed conductor, due to Li^+ and protons' mobility, and its dc intensity decays with time. This exchanged sample shows a higher conductivity ($10^{-3}\ \Omega^{-1}$ cm at 845 K). The ac experimental results have been fitted to an equivalent circuit by a non-linear square method (Boukamp). The Nyquist

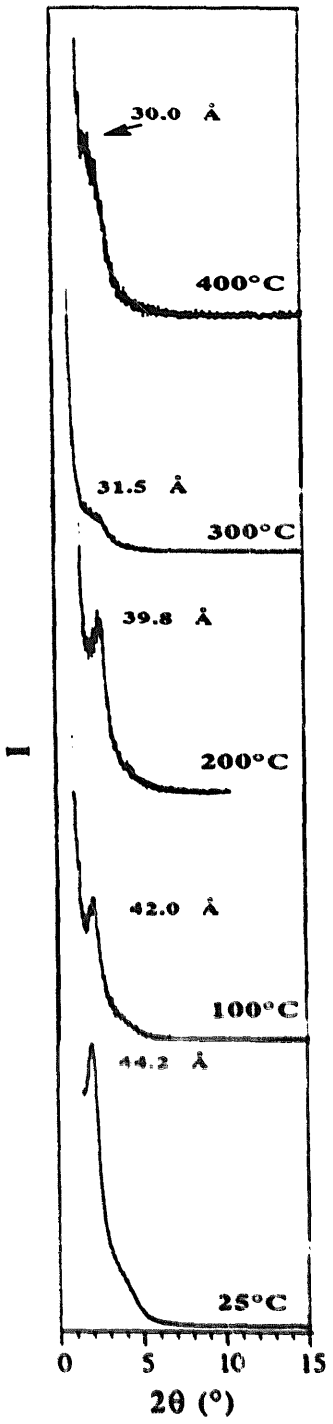

Fig. 1. X-ray low angle diffraction patterns of chromia-pillared zirconium phosphate at different temperatures.

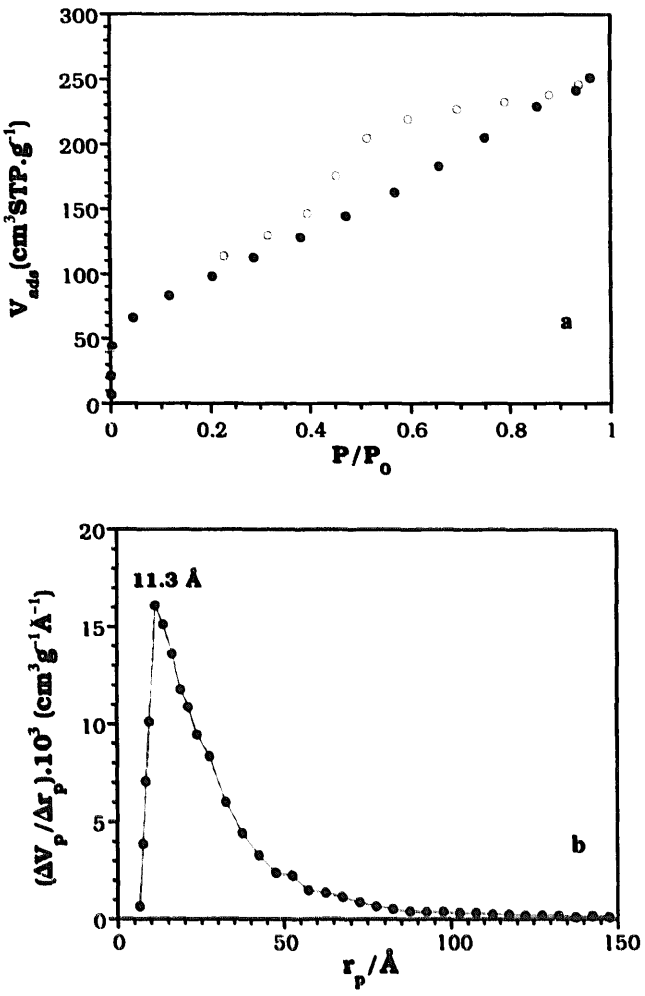

Fig. 2. (a) N_2 adsorption-desorption isotherm at 77 K and (b) pore size distribution of chromia-pillared zirconium phosphate obtained at 400°C.

plots and their equivalent circuits obtained for the pure chromia-pillared and for the Li^+-exchanged sample are very different. The first sample presents a simple depressed semicircle (Fig. 3); whereas, the corresponding plot of the Li^+-exchanged sample shows a depressed semicircle at low frequencies with a tail at higher frequencies (Fig. 4). The equivalent circuit for the pure chromia pillared sample is, in the Boukamp notation, for all temperatures, $R(RQ)$ where Q is a constant phase element (CPE), being a characteristic circuit for non-blocking electrodes. The first resistance represents the resistance for an infinite frequency and is due to the bulk resistance, the other one is due to the grain boundary effects. However, the equivalent circuit for the Li^+-exchanged sample changes with temperature and in all cases presents a blocking electrode diagram. At low temperature we can observe two relaxation processes; the lowest frequency relaxation is attributed to a capacity and resistance between grain boundaries, and the highest frequency relaxation is due to the bulk processes; however, at high temperature there is no indication of a grain boundary effect in the impedance diagram.

Measurement of ac conductivity ($\sigma(\omega)$) of many materials produces a frequency independent plateau, which is usually identified with dc conductivity, while a dispersive bulk phenomena is present at high frequencies. According to Jonscher [13] the ac conductivity may be expressed:

$$\sigma'(\omega) = \sigma_{dc} + Y\omega^n \quad (1)$$

where σ_{dc} is the direct current conductivity, Y is a temperature-dependent parameter which determines the magnitude of the dispersion found at high frequencies, ω is the angular frequency of the applied field and finally, n is an experimental parameter that is in the range $0 < n < 1$ [8]. In Fig. 5, $\lg\sigma(\omega)$ versus $\lg\omega$ is plotted for the pure and Li^+-exchanged porous solids. When the carrier concentration is thermally activated, the activation energy is composed of two terms: E_a, which is associated to the hopping rate of the mobile charge carriers and E_c, which depends on the charge carriers concentration [14]. Consequently, the dc conductivity may be expressed as:

$$\sigma_{dc}T = \sigma_0\exp\{-(E_a + E_c)/kT\} \quad (2)$$

where σ_0 is a prefactor, k is the Boltzmann constant. Considering that the ion-exchanged chromic-pillared α-zirconium phosphate material is a weak electrolyte, two distinctive carrier populations, 'mobile' and 'immobile' carriers are assumed to exist. In the weak model, almost all carriers are bound at various traps and only those that relapse contribute to electrical

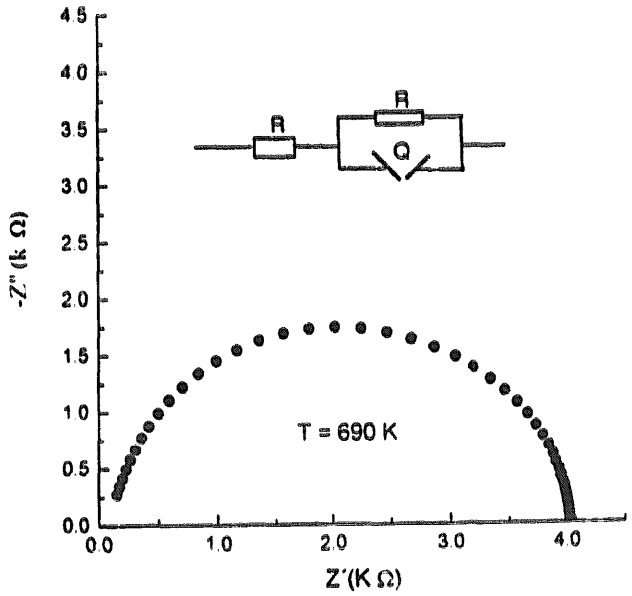

Fig. 3. 690 K Nyquist plot for chromia-pillared zirconium phosphate. Insert shows equivalent circuit.

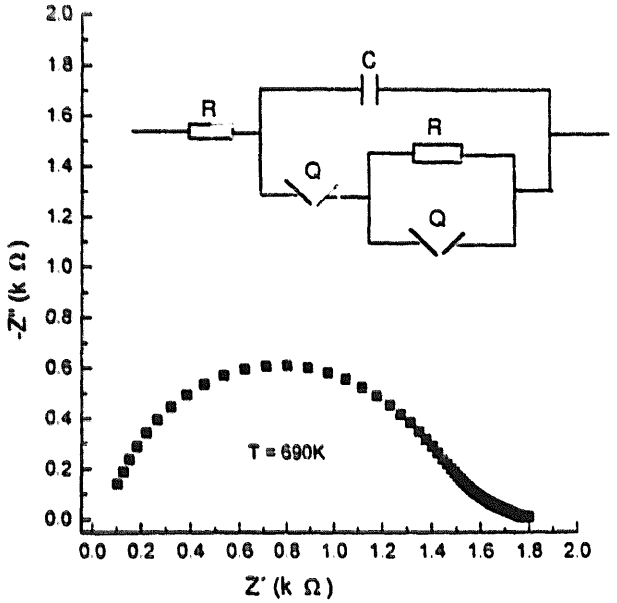

Fig. 4. 690 K Nyquist plot for Li^+-exchanged chromia-pillared zirconium phosphate. Insert shows equivalent circuit.

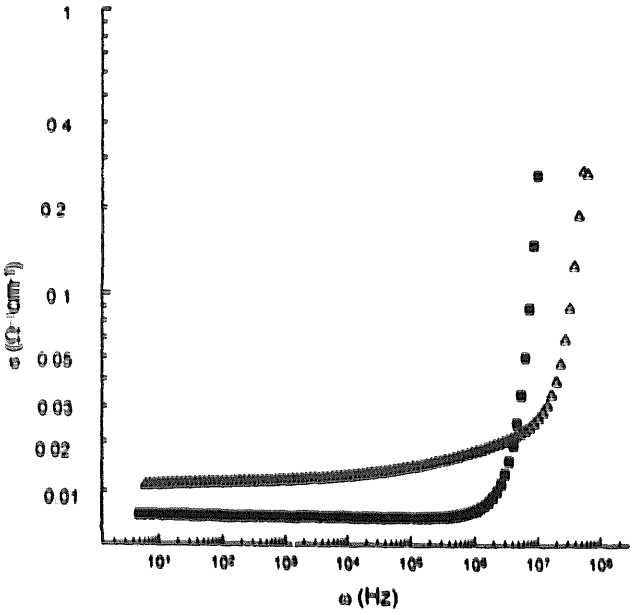

Fig. 5. Ac conductivity versus frequency for (△) Li^+-exchanged chromia-pillared zirconium phosphate, (■) chromia-pillared zirconium phosphate.

conductivity [14]. The ionic hopping frequency, which can be obtained directly from ac conductivity data [14], depends only on the activation energy E_a. It corresponds to the frequency where the electrical conductivity changes from low to high frequency dispersion regime, and is being expressed as a simple Arrhenius plot

$$\omega_p = \omega_e \exp(-E_a/k) \quad (3)$$

Table 1
Activation energies and effective attempt frequencies of the samples studied

	Chromia-pillared-ZrP	Li^+-chromia-pillared-ZrP
E_a (eV)	0.33	0.66
E_c (eV)	0.1	0.26
ω_e (MHz)	4.1	5.6

Here, ω_e is the effective attempt frequency of the ion moving from its site to the nearest neighbouring site [14].

Fig. 6 shows the Arrhenius plot for dc current and the characteristic frequency for the two samples. In all cases, for the dc conductivity, hopping frequency and charge carrier concentration, the respective activation energies for the pure chromia-pillared α-zirconium phosphate are lower than the Li^+-exchanged derivative sample. Table 1 shows the activation energies and the effective attempt frequency for both samples. The pure chromia-pillared zirconium phosphate has an activation energy value of 0.33 eV, typical of an electronic conductor and much lower than those observed for other oxide-pillared phosphates (1.0–1.3 eV). The higher conductivity and the lower activation energy can be explained by the existence of Cr(III) and Cr(V) as demonstrated by UV-visible-NIR diffuse reflectance spectroscopy. The additional presence of Cr(V) is indicated by the transition observed at 485 nm and the existence of a low-energy broad band in the near-IR region (Pérez-Reina et al., unpublished results). The couple Cr(III)

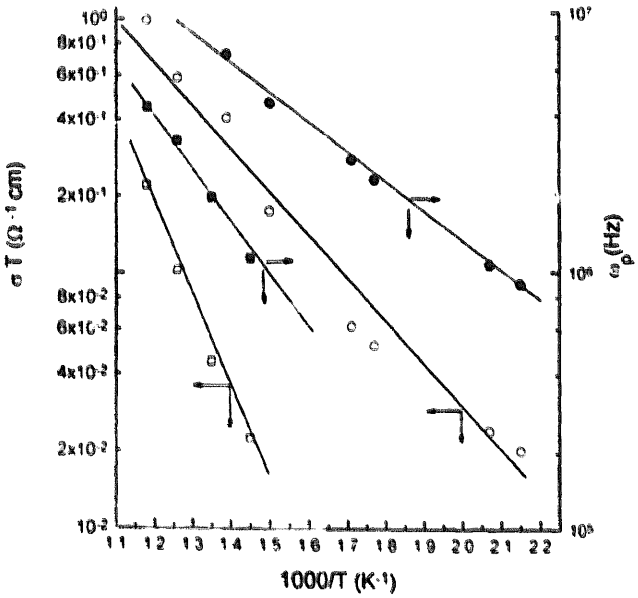

Fig. 6. Arrhenius plots for (○ σT, ●) Li^+-exchanged chromia-pillared zirconium phosphate, (□ σT, ■ ωp) chromia-pillared zirconium phosphate.

and Cr(V) facilitates the electron mobility along the structure. Li^+-exchanged chromia-pillared zirconium phosphate has an activation energy of 0.66 eV, higher than that of the unexchanged sample. This difference is due to a modification of the potential well produced by lithium ions.

References

[1] C.A.C. Sequeira, M.J. Hudson (Eds.), Multifunctional Mesoporous Inorganic Solids, NATO ASI, Kluwer Academic, Dordrecht, 1993, p. 400.

[2] I.V. Mitchell (Ed.), Pillared Layered Structures, Current Trends and Applications, Elsevier, London, 1990.

[3] G. Alberti, in: A. Clearfield (Ed.), Inorganic Ion-Exchange Materials, CRC Press, Boca Raton, FL, 1982.

[4] U. Costantino, in: A. Clearfield (Ed.), Inorganic Ion-Exchange Materials, CRC Press, Boca Raton, FL, 1982, pp. 111–132 and references therein.

[5] A. Clearfield, Chem. Rev. 88 (1988) 125.

[6] P. Olivera-Pastor, P. Maireles-Torres, E. Rodríguez-Castellón, et al., Chem. Mater. 8 (1996) 1758.

[7] C. Criado, J.R. Ramos-Barrado, P. Maireles-Torres, P. Olivera-Pastor, E. Rodríguez-Castellón, A. Jiménez-López, Solid State Ionics 61 (1993) 139.

[8] C. Criado, J.R. Ramos-Barrado, P. Maireles-Torres, P. Olivera-Pastor, A. Jiménez-López, E. Rodríguez-Castellón, Mater. Res. Soc. Symp. Proc. 286 (1993) 347.

[9] J.R. Ramos-Barrado, C. Criado, P. Maireles-Torres, P. Olivera-Pastor, E. Rodríguez-Castellón, A. Jiménez-López, Solid State Ionics 73 (1994) 67.

[10] J.R. Ramos-Barrado, C. Criado, P. Maireles-Torres, P. Olivera-Pastor, E. Rodríguez-Castellón, A. Jiménez-López, Mater. Res. Soc. Symp. Proc. 371 (1995) 175.

[11] J.R. Ramos-Barrado, F. Martin, E. Rodríguez-Castellón, A. Jiménez-López, P. Olivera-Pastor, F. Pérez-Reina, Solid State Ionics 97 (1997) 187.

[12] G. Alberti, E. Torraca, J. Inorg. Nucl. Chem. 30 (1968) 317.

[13] J. Jonsher, Dielectric Relaxation in Solids, Dielectric Press, Chelsea, 1983.

[14] D.P. Almond, G.K. Duncan, A.R. West, Solid State Ionics 8 (1983) 159.